THE JOURNAL OF BIOLOGICAL CHEMISTRY
Vol. 275, No. 28, Issue of July 14, pp. 21555–21565, 2000

*Printed in U.S.A.*

# Stomachs of Mice Lacking the Gastric H,K-ATPase α-Subunit Have Achlorhydria, Abnormal Parietal Cells, and Ciliated Metaplasia*

Received for publication, February 24, 2000, and in revised form, April 7, 2000
Published, JBC Papers in Press, April 10, 2000, DOI 10.1074/jbc.M001558200

**Zachary Spicer‡, Marian L. Miller§, Anastasia Andringa§, Tara M. Riddle‡, John J. Duffy‡¶, Thomas Doetschman‡, and Gary E. Shull‡‖**

*From the Departments of ‡Molecular Genetics, Biochemistry, and Microbiology and §Environmental Health, The University of Cincinnati College of Medicine, Cincinnati, Ohio 45267-0524*

**The H,K-ATPase of the gastric parietal cell is the most critical component of the ion transport system mediating acid secretion in the stomach. To study the requirement of this enzyme in the development, maintenance, and function of the gastric mucosa, we used gene targeting to prepare mice lacking the α-subunit. Homozygous mutant (*Atp4a*$^{-/-}$) mice appeared healthy and exhibited normal systemic electrolyte and acid-base status but were achlorhydric and hypergastrinemic. Immunocytochemical, histological, and ultrastructural analyses of *Atp4a*$^{-/-}$ stomachs revealed the presence of chief cells, demonstrating that the lack of acid secretion does not interfere with their differentiation. Parietal cells were also present in normal numbers, and despite the absence of α-subunit mRNA and protein, the β-subunit was expressed. However, *Atp4a*$^{-/-}$ parietal cells had dilated canaliculi and lacked typical canalicular microvilli and tubulovesicles, and subsets of these cells contained abnormal mitochondria and/or massive glycogen stores. Stomachs of adult *Atp4a*$^{-/-}$ mice exhibited metaplasia, which included the presence of ciliated cells. We conclude that ablation of the H,K-ATPase α-subunit causes achlorhydria and hypergastrinemia, severe perturbations in the secretory membranes of the parietal cell, and metaplasia of the gastric mucosa; however, the absence of the pump appears not to perturb parietal cell viability or chief cell differentiation.**

Secretion of hydrochloric acid in the stomach is dependent on the gastric H,K-ATPase, a P-type ATPase that is present in tubulovesicular and canalicular membranes of the gastric parietal cell. The enzyme consists of two subunits (1–3), a 114-kDa α-subunit (gene locus *Atp4a*) and a 35-kDa (protein moiety) β-subunit (gene locus *Atp4b*). The α-subunit contains ATP and cation binding sites and carries out the catalytic and transport functions of the enzyme (1), and it also contains sequences responsible for apical membrane localization (4). The heavily glycosylated β-subunit is required for endocytic retrieval of the H,K-ATPase from the canilicular membranes as the cell passes from the stimulated to the resting state (5) and may also contribute to proper folding and membrane localization of the enzyme (1).

When the resting parietal cell is stimulated by acid secretogogues, the tubulovesicles are transformed into the secretory canaliculus (6). HCl (~160 mM) and KCl (~17 mM) are then secreted via the combined activities of the H,K-ATPase, which mediates the electroneutral exchange of intracellular $H^+$ and extracellular $K^+$, and both $K^+$ and $Cl^-$ channels, which allow the passage of these ions down their electrochemical gradients. Because it is a major component of the tubulovesicular and canalicular membranes, it is possible that the H,K-ATPase is necessary for the biosynthesis and/or integrity of these membranes, and it might also play a role in the reversible transformations from one membrane state to the other via interactions with cytoskeletal components and other proteins. The recently described phenotype of a mouse lacking the gastric H,K-ATPase β-subunit (7), in which there were severe perturbations of the tubulovesicular and canalicular membrane systems, is consistent with this hypothesis.

There are indications that the acid secretory activity of the H,K-ATPase might be necessary for the viability and normal development of parietal cells (8) and possibly for the differentiation of chief cells (9). A frequent observation in gastric glands of animals treated with inhibitors of acid secretion is the presence of parietal cells with dilated canaliculi or vacuoles (8, 10–12). Treatment with omeprazole, an inhibitor of the H,K-ATPase, caused degeneration of parietal cells and an expansion of the number of preparietal cells, and it also caused a reduction in the number of mature chief cells (8, 9). Expression of diphtheria toxin (13) or simian virus 40 large T antigen (14) in parietal cells of transgenic mice caused the loss of mature parietal cells, an expansion of the preparietal cell population, and an apparent block in the maturation of chief cells. Li *et al.* (14) suggested that the inhibition of chief cell maturation might be secondary to the accompanying defect in acid secretion or, alternatively, that the parietal cell might play a direct role in controlling the differentiation and maturation of gastric epithelial cell types.

Although the function of the gastric H,K-ATPase in acid secretion is well established, the importance of its acid secretory activity for the viability of the parietal cell and for the normal development of the gastric mucosa is not well understood. On the basis of studies discussed above, it seems likely that gastric H,K-ATPase activity might be a critical factor in the development and maintenance of parietal cells and other cells of the gastric mucosa. To address this issue, we have developed and analyzed a mouse model in which expression of the H,K-ATPase α-subunit mRNA and protein was eliminated. Our studies show that there are significant differences between the histopathology that occurs in the gastric mucosa of mice lacking the H,K-ATPase α-subunit and that observed after

* This work was supported by National Institutes of Health Grant DK50594. The costs of publication of this article were defrayed in part by the payment of page charges. This article must therefore be hereby marked "*advertisement*" in accordance with 18 U.S.C. Section 1734 solely to indicate this fact.

¶ Deceased.

‖ To whom correspondence should be addressed: Dept. of Molecular Genetics, Biochemistry and Microbiology, University of Cincinnati, College of Medicine, 231 Bethesda Ave., Cincinnati, OH 45267-0524. Tel.: 513-558-0056; Fax: 513-558-1885; E-mail: shullge@ucmail.uc.edu.

treatment with H,K-ATPase inhibitors or elimination of the H,K-ATPase β-subunit (7).

## EXPERIMENTAL PROCEDURES

*Preparation of Targeting Construct*—A portion of the gastric H,K-ATPase gene was isolated from a mouse strain 129/SvJ phage genomic library using a rat gastric H,K-ATPase cDNA probe. The clone was partially characterized by restriction mapping, Southern blot analysis, polymerase chain reaction, and DNA sequencing. Exons 4, 7, 16, 19, and 20 were amplified by polymerase chain reaction, and DNA sequence analysis showed that they matched the published mouse cDNA sequence (15). A polymerase chain reaction strategy was used to obtain fragments for insertion into the MJK$^+$KO (16) targeting vector. The 3.4-kb[1] 5′ arm extended from codon 71 in exon 4 to codon 359 in exon 8. The 3.4-kb 3′ arm extended from codon 390 in exon 8 to codon 600 in exon 13. Initial subcloning of the arms into the targeting vector resulted in rearrangements of the plasmid, most likely due to the presence of poison sequences in the genomic fragments, with subsequent selection of rearrangements during growth of the bacteria harboring the plasmid. Therefore, the targeting vector was modified by replacing the portion of the vector containing pBluescript plasmid sequences with the pBR322 plasmid, which converted the targeting vector to a low copy plasmid. Also, *Not*I, *Pac*I, *Hin*dIII, and *Asc*I cloning sites were added to the vector immediately 5′ of the neomycin resistance gene. The 3′ arm was blunt end-ligated into the *Not*I site, and the 5′ arm was blunt end-ligated into the *Xho*I site between the neomycin resistance and herpes simplex virus thymidine kinase genes. This strategy resulted in the replacement of 31 codons with the neomycin resistance gene.

*Gene Targeting and Generation of Mutant Animals*—Electroporation of the targeting construct, after linearizing with *Pac*I, into ES cells and selection of G418- and gancyclovir-resistant ES cell lines were carried out as described previously (16). ES cell lines that underwent homologous recombination were identified by Southern blot analysis using a 0.6-kb probe that consisted of a genomic fragment extending from codon 26 in exon 2 to codon 70 in exon 4. Chimeric mice were generated by blastocyst-mediated transgenesis and mated to Black Swiss mice. Offspring with ES cell-derived genetic material were identified by their agouti coat color, and those carrying the targeted allele were determined by Southern blot analysis of tail DNAs using a genomic probe extending from codon 418 in exon 9 to codon 559 in exon 11.

*Analysis of Blood Gases and Electrolytes*—Awake mice were gently warmed for 10–15 min on a heating pad to increase peripheral blood circulation. Blood (50 μl) from the tail vein was collected in heparin-treated capillary tubes and analyzed immediately for gases, electrolytes, and pH using a Chiron diagnostics model 348 pH/blood gas analyzer (Chiron, Norwood, MA).

*Acid-Base Equivalents and pH of Stomach Contents*—pH and acid-base equivalents of the gastric contents were measured as described previously with slight modifications (16, 17). Sex-matched mice of all three genotypes (8–10 weeks old) were fasted for 2 h prior to the experiment. Histamine HCl in phosphate-buffered saline was injected subcutaneously (2 μg/g body weight; Sigma Chemical Co., St. Louis, MO). After 45 min, the mice were killed, and their stomachs were removed. Stomach contents were emptied into 2 ml of $N_2$-saturated normal saline, insoluble material was pelleted by centrifugation, and the pH of the supernatant was measured. The supernatant was then titrated to pH 6.5 (pH of normal saline) with either 0.01 N NaOH or 0.01 N HCl, and the data were expressed as microequivalents per gram of wet stomach weight.

*Serum Gastrin Determination*—Mice of all three genotypes, 8–12 weeks old, were fasted overnight and anesthetized with avertin, and blood was collected by cardiocentesis. Serum was prepared, and gastrin concentrations were determined using an $^{125}$I radioimmunoassay kit (Diagnostic Products Corp.) as described previously (16).

*Northern Blot Analysis*—Total RNA was isolated from the stomachs of *Atp4a*$^{+/+}$, *Atp4a*$^{+/-}$, and *Atp4a*$^{-/-}$ mice using Tri-Reagant (Molecular Research Center, Inc., Cincinnati, OH). RNA was denatured with glyoxal, separated by electrophoresis in a 1% agarose gel, and transferred to a nylon membrane. The following probes were sequentially hybridized with the blot using the method of Church and Gilbert (18): rat gastric H,K-ATPase α-subunit, rat gastric H,K-ATPase β-subunit, rat pepsinogen C, rat intrinsic factor, rat gastrin, and mouse L32 ribosomal subunit as a loading control. Blots were analyzed by autoradiography and PhosphorImager analysis (Molecular Dynamics, Inc., Sunnyvale, CA).

*Immunohistochemistry*—Antibodies and lectin and the dilutions for each used in immunohistochemical analysis of stomach sections were as follows: rabbit anti-α-subunit of porcine gastric H,K-ATPase (1:100; Calbiochem-Novabiochem); rabbit anti-β-subunit of porcine gastric H,K-ATPase (1:25; Calbiochem-Novabiochem); sheep anti-human pepsinogen II (1:25; Biodesign International, Kennebunk, ME); donkey anti-rabbit IgG (1:100; Cortex Biochem, Inc., San Leandro, CA); donkey anti-sheep IgG (1:100; Cortex Biochem, Inc., San Leandro, CA); and fluorescein isothiocyanate-conjugated *Dolichos biflorus* agglutinin (40 μg/ml; Sigma). The secondary antibodies were conjugated to Texas Red fluorophore. For immunohistochemical staining, stomachs were removed from 10-week-old mice, fixed in 10% neutral buffered formalin, and embedded in paraffin. Sections (5 μm) were cut, deparaffinized with xylene, and rehydrated with graded concentrations of ethanol. Slides that were stained with antibodies were first blocked with normal donkey serum. The primary antibodies, diluted in normal donkey serum, were incubated overnight at 4 °C, while the secondary antibodies were incubated in the dark for 1 h at room temperature. The lectin, *D. biflorus* agglutinin, was diluted in phosphate-buffered saline with 1% bovine serum albumin and 0.3% Triton X-100. Stomach sections treated with *D. biflorus* agglutinin were first blocked with phosphate-buffered saline containing 1% bovine serum albumin and 0.3% Triton X-100, incubated overnight with the lectin at 4 °C, and washed three times in phosphate-buffered saline.

*Microscopy and Morphometry*—Stomachs were removed from juvenile (17-day-old, $n$ = 2 wild-type, 2 heterozygous, and 2 homozygous mutant) and adult (10–12-week-old, $n$ = 4 wild-type, 2 heterozygous, and 4 homozygous mutant) mice, fixed in 10% neutral buffered formalin, and embedded in paraffin. Blocks were cut into 5-μm-thick sections and stained with either hematoxylin and eosin or periodic acid-Schiff (PAS) and Alcian blue for examination by light microscopy. Stomachs from another set of juvenile ($n$ = 4 wild-type, 1 heterozygous, and 4 homozygous mutant) and adult ($n$ = 4 wild-type, 3 heterozygous, and 4 homozygous mutant) mice were fixed in 4% paraformaldehyde in phosphate buffer (pH 7.3), embedded in Spurr's resin, sectioned 1 μm thick, and stained with toluidine blue for detailed light microscopy. Sections from the same wild-type and homozygous mutants ($n$ = 4 of each genotype), 0.9 μm thick, were stained with uranyl acetate and lead citrate and examined by electron microscopy.

Morphometry was performed as described previously (16) using 17-day-old (two of each genotype) and 10–12-week-old (four of each genotype) wild-type and null mutant mice. Only cells in which the nucleus was present in the plane of section were counted. Using phase contrast, all cells in the normal position of parietal cells in the gastric gland and having features typical of parietal cells (*e.g.* canaliculi or numerous and large mitochondria) were counted as parietal cells, regardless of whether their morphology was normal. Cells located in the base or neck of the gland and having at least six large birefringent granules were counted as chief cells. Cells with small apical mucous granules in the neck of the gastric gland and cells at the gastric pit and surface were counted as mucous cells. Cells without distinguishing features, such as secretory granules or large mitochondria or canaliculi, were counted as "other" cells.

## RESULTS

*Generation of Atp4a$^{-/-}$ Mice*—The mutant allele of *Atp4a* was generated in ES cells by replacing codons 360–390 in exon 8 with the neomycin resistance gene (Fig. 1, *A* and *B*). The region that was deleted encodes sequences extending from the fourth transmembrane domain to just beyond the conserved phosphorylation site (Asp$^{385}$), which is required for enzyme activity. This region was eliminated to ensure that the mutant allele would be functionally null. Chimeric mice were generated using one of the targeted ES cell lines, and the null allele was successfully transmitted through the germ line. Southern blot analysis of tail DNA samples from litters of heterozygous matings (Fig. 1*C*) demonstrated that mice of all three genotypes were born in the expected Mendelian ratios (102 +/+, 172 +/−, and 99 −/−). *Atp4a$^{-/-}$* mice thrived, were indistinguishable from their wild-type and heterozygous littermates in both behavior and outward appearance, and were fertile.

*Systemic Acid/Base and Electrolyte Status*—The α-subunit

[1] The abbreviations used in this paper are: kb, kilobase pair(s); ES, embryonic stem; PAS, periodic acid-Schiff; *Atp4a$^{-/-}$*, *Atp4a$^{+/-}$*, and *Atp4a$^{+/+}$*, gastric H,K-ATPase α-subunit homozygous mutant, heterozygous mutant, and wild-type, respectively.

of the gastric H,K-ATPase is expressed in mouse kidney (19), and it has been suggested that it might function in renal control of acid-base or potassium homeostasis (20). As an initial test of this hypothesis, blood samples were taken from adult animals of all three genotypes, and plasma electrolytes, blood pH, and blood gasses were analyzed. As shown in Table I, no significant differences were observed among the three genotypes.

*Atp4a*$^{-/-}$ *Mice Are Achlorhydric and Hypergastrinemic*—To confirm that the gastric H,K-ATPase is solely responsible for gastric acid secretion and to determine whether the loss of one copy of the gastric H,K-ATPase α-subunit gene leads to a reduction in net acid secretion, we measured the pH and acid-base content of gastric secretions from histamine-treated *Atp4a*$^{+/+}$, *Atp4a*$^{+/-}$, and *Atp4a*$^{-/-}$ mice. The contents of *Atp4a*$^{+/+}$ and *Atp4a*$^{+/-}$ stomachs were similar with respect to both pH (3.17 ± 0.17 and 3.13 ± 0.21, respectively; Fig. 2*A*) and acid equivalents (35.4 ± 9.0 μeq/g and 32.5 ± 5.2 μeq/g, respectively; Fig. 2*B*). In contrast, the pH of the gastric contents of *Atp4a*$^{-/-}$ mice was close to neutrality (6.9 ± 0.1; Fig. 2*A*) and contained net base (4.5 ± 2.3 μeq base/g; Fig. 2*B*).

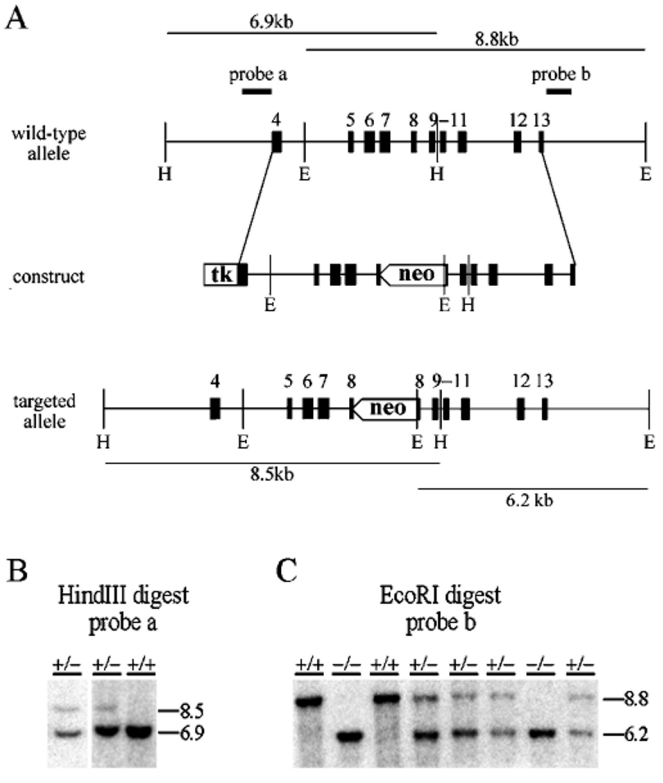


FIG. 1. **Gastric H,K-ATPase α-subunit gene targeting and Southern blot analysis.** *A*, gene targeting strategy. *Top*, genomic structure showing exons 4–13; *middle*, targeting construct, with neomycin resistance gene replacing 31 codons in exon 8; *bottom*, structure of gene after homologous recombination. *tk*, herpes simplex virus thymidine kinase gene used for negative selection. *H*, *Hin*dIII; *E*, *Eco*RI. The 6.9-kb *Hin*dIII and 8.8-kb *Eco*RI fragments present in the wild-type allele are shown *above*, and the 8.5-kb *Hin*dIII and 6.2-kb *Eco*RI fragments present in the mutant allele are shown *below*. The probes used to distinguish between wild-type and mutant alleles after digestion with *Hin*dIII (probe a) or *Eco*RI (probe b) are *indicated. B*, Southern blot analysis of DNA isolated from ES cells after electroporation with targeting construct and selection with gancyclovir and G418. DNA was digested with *Hin*dIII and hybridized with probe a. *C*, Southern blot genotyping of offspring from a heterozygous mating. DNA from tail biopsies was digested with *Eco*RI and hybridized with probe b.

The peptide hormone gastrin is known to play an important role in the regulation of acid secretion (21) and is induced in several mouse models of achlorhydria (7, 16) or hypochlorhydria (22). Northern blot analysis showed that gastrin mRNA was increased ~4-fold in *Atp4a*$^{-/-}$ stomachs compared with *Atp4a*$^{+/+}$ or *Atp4a*$^{+/-}$ stomachs (Fig. 3*A*). In addition, serum gastrin concentrations (Fig. 3*B*) were significantly higher in *Atp4a*$^{-/-}$ mice than in either heterozygous or wild-type mice (*Atp4a*$^{-/-}$, 499 ± 120 pg/ml; *Atp4a*$^{+/-}$, 131 ± 45 pg/ml; *Atp4a*$^{+/+}$, 81 ± 21 pg/ml).

*Northern Blot Analysis of H,K-ATPase, Intrinsic Factor, and Pepsinogen mRNA*—High levels of the gastric H,K-ATPase α-subunit mRNA were present in *Atp4a*$^{+/+}$ stomachs, and there was little, if any, decrease in *Atp4a*$^{+/-}$ stomachs (Fig. 4, *top panel*). Although trace levels of an ~1-kb mRNA were detected in samples from *Atp4a*$^{-/-}$ stomachs after long autoradiographic exposures (data not shown), the wild-type mRNA was absent in the knockout (Fig. 4, *top panel*). In contrast, mRNA for the H,K-ATPase β-subunit was ~1.8-fold more abundant in the *Atp4a*$^{-/-}$ samples than in the *Atp4a*$^{+/+}$ or *Atp4a*$^{+/-}$ samples (Fig. 4, *second panel*).

In the rodent stomach, pepsinogen and intrinsic factor are expressed almost exclusively in chief cells (23, 24), making them excellent molecular markers for this cell type. In the *Atp4a*$^{-/-}$ stomach, intrinsic factor mRNA was detected at levels comparable with those observed in *Atp4a*$^{+/+}$ and *Atp4a*$^{+/-}$ stomachs (Fig. 4, *third panel*), suggesting that mature chief cells were present. Pepsinogen mRNA, however, was sharply reduced in the *Atp4a*$^{-/-}$ stomachs (Fig. 4, *fourth panel*).

*Immunohistochemical Analyses Reveal β-Subunit Protein, Pepsinogen, and Abundant Parietal and Chief Cells in Atp4a*$^{-/-}$ *Stomachs*—As noted above, the α-subunit probe, which corresponded to the N-terminal coding sequence, detected trace amounts of a 1-kb mRNA in *Atp4a*$^{-/-}$ stomachs. To address the possibility that a stable protein containing N-terminal sequences might be translated from the aberrant transcript and to further document the null mutation, immunocytochemistry of stomach sections was performed using an antibody directed against a peptide sequence from the N terminus of the protein. Parietal cells of adult *Atp4a*$^{+/+}$ mice were heavily stained (Fig. 5*A*), but no specific staining was detected in *Atp4a*$^{-/-}$ parietal cells (Fig. 5*B*).

To determine whether β-subunit protein was present in *Atp4a*$^{-/-}$ stomachs, as suggested by the abundance of its mRNA, and to assess the relative numbers of parietal cells in stomachs of wild-type and mutant mice, stomach sections were stained with an antibody directed against the gastric H,K-ATPase β-subunit and with *D. biflorus* agglutinin, both of which have been used as parietal cell markers (23). In both *Atp4a*$^{+/+}$ and *Atp4a*$^{-/-}$ stomachs, a comparable number of cells were stained with the β-subunit antibody (Fig. 6, *B* and *F*) and with *D. biflorus* agglutinin (Fig. 6, *D* and *H*). Staining with

TABLE I
*Plasma electrolytes and acid-base status*

All values are means ± S.E. $n = 8$ for each genotype.

| | pH | $pCO_2$ | $pO_2$ | HCO−3 | $Na^+$ | $K^+$ | $Cl^-$ |
|---|---|---|---|---|---|---|---|
| | | *mm Hg* | *mm Hg* | *mM* | *mM* | *mM* | *mM* |
| *Atp4a*$^{+/+}$ | 7.45 ± 0.01 | 35.71 ± 1.35 | 79.53 ± 1.06 | 24.55 ± 0.93 | 148.0 ± 0.7 | 6.10 ± 0.20 | 115.3 ± 1.7 |
| *Atp4a*$^{+/-}$ | 7.45 ± 0.01 | 36.66 ± 1.26 | 73.13 ± 3.32 | 24.91 ± 0.87 | 148.5 ± 0.5 | 6.02 ± 0.19 | 116.0 ± 0.8 |
| *Atp4a*$^{-/-}$ | 7.48 ± 0.04 | 35.44 ± 1.3 | 74.89 ± 3.27 | 24.06 ± 1.20 | 148.0 ± 0.6 | 6.60 ± 0.31 | 115.4 ± 0.5 |

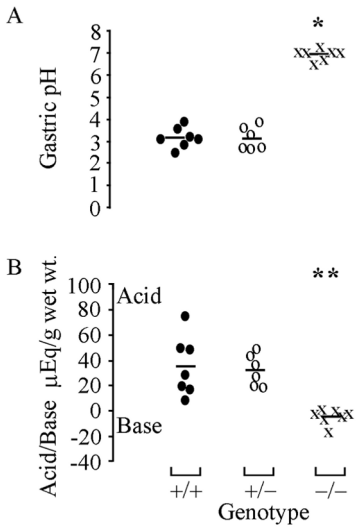


FIG. 2. **Impaired gastric acid secretion in *Atp4a*$^{-/-}$ mice.** *A*, pH of gastric secretions; *B*, acid-base content (expressed as microequivalents per g of wet stomach weight) of the stomachs of 8–10-week-old mice ($n$ = 7 *Atp4a*$^{+/+}$, 6 *Atp4a*$^{+/-}$, and 7 *Atp4a*$^{-/-}$). Samples were collected 45 min after subcutaneous injection of histamine HCl. The genotypes are indicated *below*, and the mean for each measurement is indicated by a *horizontal bar*. *, $p < 0.001$; **, $p < 0.005$ for difference between *Atp4a*$^{-/-}$ and *Atp4a*$^{+/+}$ mice as determined by analysis of variance-protected Bonferroni's $t$ test.

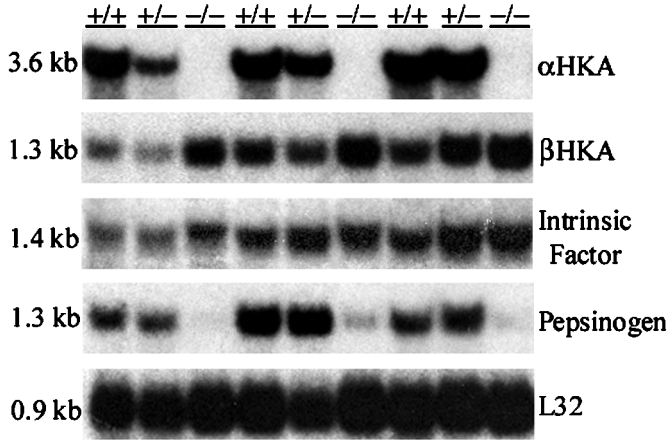


FIG. 4. **Northern blot analysis of stomach RNA.** Total stomach RNA (10 μg) from 8-week-old *Atp4a*$^{+/+}$, *Atp4a*$^{+/-}$, and *Atp4a*$^{-/-}$ mice was hybridized with probes for mRNAs expressed in parietal cells (H,K-ATPase α and β subunit mRNAs) and chief cells (intrinsic factor and pepsinogen mRNAs). The L32 ribosomal subunit mRNA served as loading control. Note that H,K-ATPase α-subunit (*αHKA*) mRNA was eliminated in *Atp4a*$^{-/-}$ stomachs and that expression of H,K-ATPase β-subunit (*βHKA*) mRNA was up-regulated 1.8-fold (determined by PhosphorImager analysis) in the *Atp4a*$^{-/-}$ stomachs. The amount of intrinsic factor mRNA was approximately the same in all three genotypes, while pepsinogen mRNA was markedly decreased in *Atp4a*$^{-/-}$ mice.

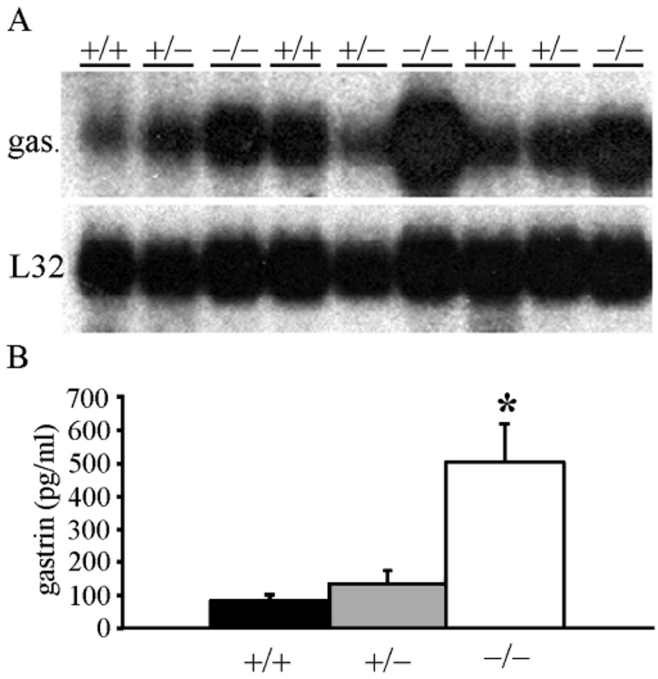


FIG. 3. **Gastrin mRNA in stomach and serum gastrin levels.** *A*, Northern blot analysis of gastrin mRNA (*top*) from stomachs of three mice of each genotype (indicated *above* each *lane*). After hybridization with a rat gastrin cDNA probe, the blot was stripped and hybridized with a mouse L32 ribosomal subunit cDNA probe as a loading control (*bottom panel*). Each *lane* contained 10 μg of total stomach RNA from an 8-week-old mouse. *B*, sera from 8-week-old mice were analyzed by radioimmune assay to determine gastrin concentrations. $n$ = 6 *Atp4a*$^{+/+}$, 5 *Atp4a*$^{+/-}$, and 12 *Atp4a*$^{-/-}$ mice. Data are expressed as mean ± S.E. *, $p < 0.03$ for difference between *Atp4a*$^{-/-}$ and either *Atp4a*$^{+/-}$ or *Atp4a*$^{+/+}$ as determined by single-factor analysis of variance.

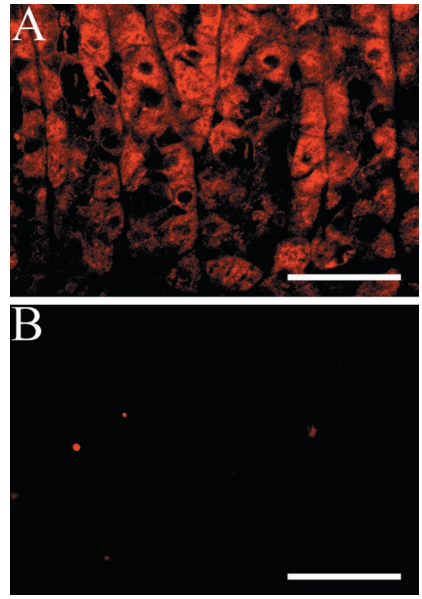


FIG. 5. **Immunofluorescent detection of gastric H,K-ATPase α-subunit in *Atp4a*$^{+/+}$ stomachs but not *Atp4a*$^{-/-}$ stomachs.** Sections from stomachs of 10-week-old *Atp4a*$^{+/+}$ (*A*) and *Atp4a*$^{-/-}$ (*B*) mice were incubated with a polyclonal antibody directed against the N-terminal sequence of the gastric H,K-ATPase α-subunit. Binding of the primary antibody was detected using Texas Red-conjugated secondary antibody. Cells in the neck and base of the gastric gland were strongly stained in *Atp4a*$^{+/+}$ stomachs (*A*) but not in *Atp4a*$^{-/-}$ stomachs (*B*). *Scale bar*, 50 μm.

the β-subunit antibody seemed less intense in *Atp4a*$^{-/-}$ sections compared with *Atp4a*$^{+/+}$ sections (Fig. 6, *B* and *F*), suggesting that β-subunit protein is present at lower levels in *Atp4a*$^{-/-}$ parietal cells than in wild-type cells, despite the higher mRNA levels. Positively staining cells in the wild-type stomach had the normal appearance of parietal cells (Fig. 6, *B* and *D*). In contrast, positively staining cells in *Atp4a*$^{-/-}$ stomachs had numerous vacuole-like structures in the cytoplasm (Fig. 6, *F* and *H*) reminiscent of the dilated canaliculi observed after treatment with omeprazole (8, 11, 12). While these cells did not exhibit normal parietal cell morphology, their staining with both the β-subunit antibody and *D. biflorus* agglutinin confirmed that they were parietal cells; this conclusion was supported by analysis of their ultrastructure.

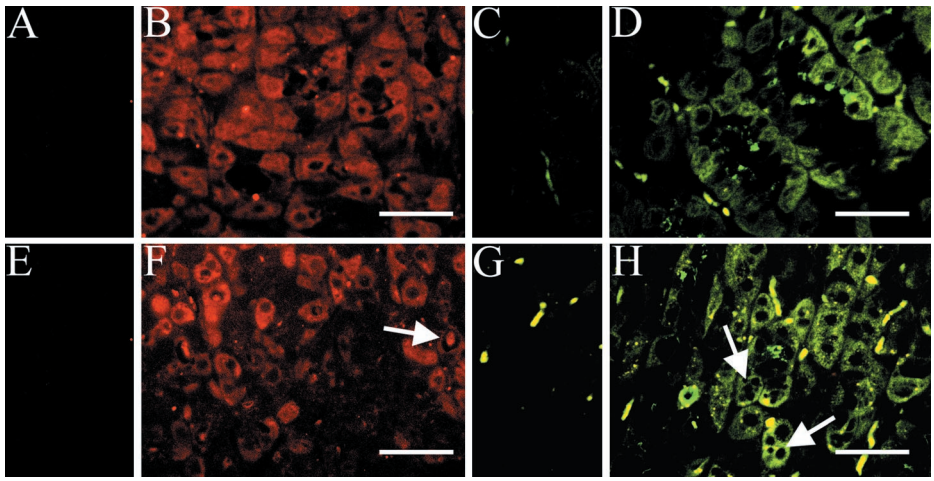


FIG. 6. **Immunofluorescent identification of parietal cells in *Atp4a*$^{+/+}$ and *Atp4a*$^{-/-}$ stomachs.** Sections from stomachs of 10-week-old *Atp4a*$^{+/+}$ (*A–D*) and *Atp4a*$^{-/-}$ (*E–H*) mice were examined for reactivity to parietal cell markers. Control sections from *Atp4a*$^{+/+}$ (*A*) and *Atp4a*$^{-/-}$ (*E*) stomachs incubated with the secondary antibody alone exhibited no specific staining. When incubated with a rabbit antibody against porcine gastric H,K-ATPase β-subunit and Texas Red-conjugated donkey anti-rabbit IgG secondary antibody, cells in both *Atp4a*$^{+/+}$ (*B*) and *Atp4a*$^{-/-}$ (*F*) sections stained positively for the gastric H,K-ATPase β-subunit. When incubated with blocking serum alone, no specific staining was observed in control sections from *Atp4a*$^{+/+}$ (*C*) and *Atp4a*$^{-/-}$ (*G*) stomachs; some degree of autofluorescence was observed. When incubated with 40 μg/ml *D. biflorus* agglutinin, both *Atp4a*$^{+/+}$ (*D*) and *Atp4a*$^{-/-}$ (*H*) sections stained positively for parietal cells. The *arrows* indicate gastric H,K-ATPase β-subunit-positive cells (*F*) and *D. biflorus* agglutinin-positive cells (*H*) with vacuole-like dilations. *Scale bar*, 50 μm.

To determine if mature chief cells containing pepsinogen stores were present in *Atp4a*$^{-/-}$ stomachs, despite the sharp decrease in pepsinogen mRNA, stomach sections from *Atp4a*$^{+/+}$ and *Atp4a*$^{-/-}$ mice were stained with an anti-pepsinogen antibody. As shown in Fig. 7, both *Atp4a*$^{+/+}$ (Fig. 7*B*) and *Atp4a*$^{-/-}$ (Fig. 7*D*) stomachs stained positive for pepsinogen, and both genotypes displayed an abundance of positively staining cells. These data, along with the normal expression of intrinsic factor mRNA, indicated that mature chief cells were present at relatively normal numbers in adult *Atp4a*$^{-/-}$ stomachs.

*Histopathologic Changes in the Gastric Mucosa of Atp4a*$^{-/-}$ *Mice*—Sections from juvenile (17-day-old) and adult (10–12-week-old) *Atp4a*$^{+/+}$ and *Atp4a*$^{-/-}$ stomachs were stained with toluidine blue and examined by light microscopy, and morphometry was performed to determine whether there were significant alterations in the numbers of gastric epithelial cell types.

Alterations in stomachs of young null mutants were mild when compared with those of adult mice. Occasional dilated gastric glands and parietal cells with vacuole-like dilations were observed in stomachs of 17-day-old *Atp4a*$^{-/-}$ mice, and enteroendocrine cells were significantly greater in numbers and in size. Both parietal and chief cells appeared to be slightly reduced in numbers (data not shown), although this may have been due to a reduced rate of maturation. The chief cells that were observed seemed to have fewer granules than those of *Atp4a*$^{+/+}$ stomachs, and the only parietal cells that could be clearly identified as such were those few that had dilated canaliculi. As discussed below, a significant reduction in parietal and chief cell numbers was not observed in adult mice, although most parietal cells were clearly abnormal, and chief cells appeared to have fewer granules.

Histopathological alterations in adult null mutants were considerably more severe than in young mice and included metaplasia (described in detail below) and a serious disruption of the architecture of the gastric gland (Fig. 8). Parietal cells in adult *Atp4a*$^{+/+}$ gastric glands were typical of those normally seen in toluidine blue-stained sections (Fig. 8*A*) and comprised 39.0 ± 1.8% of the epithelial cells in the gland (Table II). In *Atp4a*$^{-/-}$ gastric glands, cells identified as parietal cells comprised 37.8 ± 6.4% of the epithelial cells counted (Table II);

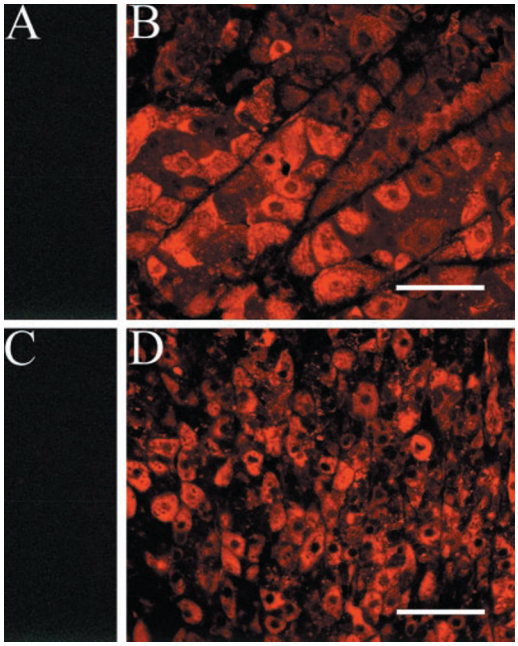


FIG. 7. **Immunofluorescent detection of pepsinogen in *Atp4a*$^{+/+}$ and *Atp4a*$^{-/-}$ stomachs.** Control sections from stomachs of 10-week-old *Atp4a*$^{+/+}$ (*A*) and *Atp4a*$^{-/-}$ (*C*) mice incubated with Texas Red-conjugated secondary antibody alone exhibited no specific staining. When incubated with a primary antibody directed against human pepsinogen II and then with the Texas Red-conjugated secondary antibody, sections from both *Atp4a*$^{+/+}$ (*B*) and *Atp4a*$^{-/-}$ (*D*) stomachs stained positively for pepsinogen. *Scale bar*, 50 μm.

however, rather than having the typical parietal cell morphology, they contained dilated caniliculi (Fig. 8, *B* and *C*), as first observed in sections stained with the β-subunit antibody and *D. biflorus* agglutinin (Fig. 6) and noted above in juvenile mice. A subset of these altered parietal cells contained massive stores of cytoplasmic glycogen. In *Atp4a*$^{+/+}$ gastric glands, glycogen-containing parietal cells comprised 0.03 ± 0.03% of the epithelial cells, while *Atp4a*$^{-/-}$ gastric glands had significantly more glycogen-containing cells (5.6 ± 0.9%; Table II).

As anticipated on the basis of immunohistochemical staining of adult stomachs with anti-pepsinogen antibodies (Fig. 7),

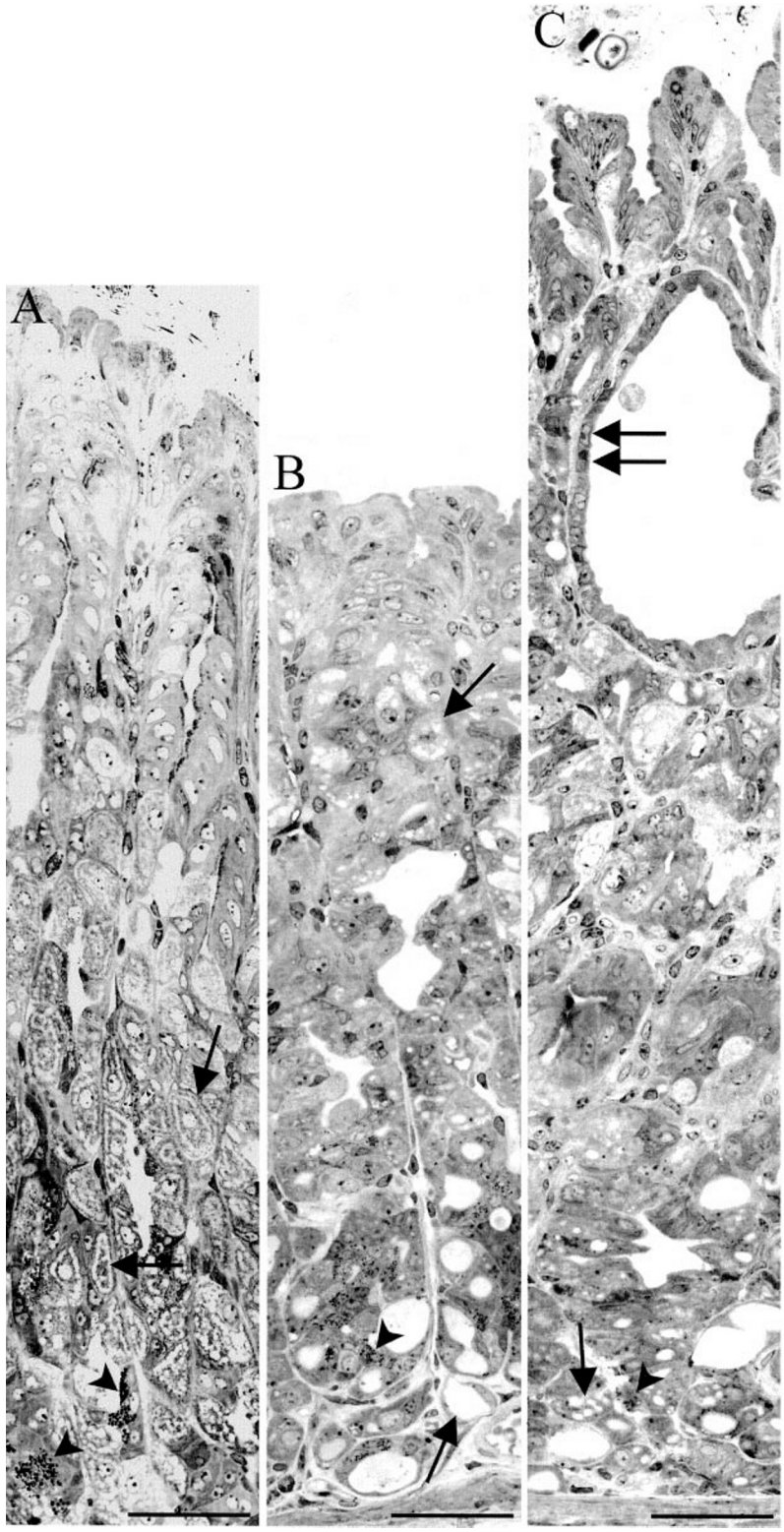


FIG. 8. **Histology of toluidine blue-stained sections of oxyntic gastric glands from *Atp4a*$^{+/+}$ and *Atp4a*$^{-/-}$ stomachs.** *A*, composite image of gastric glands from the corpus of an adult wild-type stomach. Typical parietal cells are indicated by *arrows*. Chief cells with characteristic secretory granules were present at the base of the glands (*arrowheads*). *B*, chief cells (*arrowheads*) and parietal cells (*arrows*) were also present in adult *Atp4a*$^{-/-}$ gastric glands. Parietal cells had either numerous vacuole-like dilations (*top arrow*) or a single large dilation (*bottom arrow*). *C*, severely dysplastic gastric glands from an adult *Atp4a*$^{-/-}$ mouse, with chief cells (*arrowhead*), parietal cells with cytoplasmic dilations (*arrow*), and a large cyst surrounded by a single layer of a low cuboidal epithelium (*double arrow*). *Scale bar*, = 50 $\mu$m.

chief cells with darkly staining secretory granules were visible in toluidine blue-stained sections from both *Atp4a*$^{+/+}$ (Fig. 8*A*) and *Atp4a*$^{-/-}$ (Fig. 8, *B* and *C*) gastric glands. As in juvenile mutant mice, chief cells in adult mutants appeared to have a reduced number of granules, and the lighter shading of the cytoplasm observed in toluidine blue-stained sections suggested a reduction in the amount of rough endoplasmic reticulum. Chief cells comprised 15.2 ± 2.1 and 12.0 ± 1.8% of the epithelial cells in *Atp4a*$^{+/+}$ and *Atp4a*$^{-/-}$ gastric glands, respectively (Table II). Although the mean value for the number of chief cells in *Atp4a*$^{-/-}$ mice was slightly less than in *Atp4a*$^{+/+}$ mice, the difference was not statistically significant. Also, it should be noted that the apparent reduction in the number of granules in *Atp4a*$^{-/-}$ chief cells could have led to an undercount of these cells in the null mutant, since possible chief cells containing less than six birefringent granules were included in "other" cell types.

Neither the proportion of mucous cells (*Atp4a*$^{+/+}$, 43.5 ±

TABLE II
*Epithelial cell populations of gastric glands*

Data were collected from toluidine blue-stained plastic sections. Values for each cell type are means ± S.E. and represent the percentage of the total epithelial cell population. $n = 4$ for $Atp4a^{+/+}$; $n = 4$ for $Atp4a^{-/-}$.

| Cell type | +/+ | −/− |
|---|---|---|
| Total Parietal | 39.0 ± 1.8 | 37.8 ± 6.4 |
| Glycogen[a] | 0.03 ± 0.03 | 5.6 ± 0.9[b] |
| Chief | 15.2 ± 2.1 | 12.0 ± 1.8 |
| Mucous | 43.5 ± 1.9 | 41.2 ± 3.5 |
| Enteroendocrine | 0.6 ± 0.2 | 1.9 ± 0.4[b] |
| Ciliated | 0 | 1.1 ± 0.5[b] |
| Mitotic | 0.10 ± 0.06 | 0.14 ± 0.06 |
| Other | 2.6 ± 1.4 | 9.1 ± 2.1[b] |
| Glandular thickness (μm) | 400.4 ± 20.5 | 417.0 ± 34.5 |
| Epithelial thickness (μm) | 14.6 ± 0.6 | 8.9 ± 1.2[b] |

[a] A subset of parietal cells with visible pools of glycogen.
[b] $p < 0.05$.

1.9%; $Atp4a^{-/-}$, 41.2 ± 3.5%) nor the proportion of mitotic cells ($Atp4a^{+/+}$, 0.10 ± 0.06%; $Atp4a^{-/-}$, 0.14 ± 0.06%) differed significantly between the two genotypes (Table II). The proportion of enteroendocrine cells was increased significantly in the $Atp4a^{-/-}$ glands ($Atp4a^{+/+}$, 0.61 ± 0.15%; $Atp4a^{-/-}$, 1.91 ± 0.43%). Undifferentiated cells and cells not identifiable as a specific gastric cell type (classified as "other") were increased by ~3.5-fold in $Atp4a^{-/-}$ glands ($Atp4a^{+/+}$, 2.6 ± 1.4%; $Atp4a^{-/-}$, 9.1 ± 2.1%; Table II). At least part of the increase in "other" cell types was due to the presence of what may have been immature parietal cells, since some of these cells contained numerous mitochondria but lacked canalicular membranes.

No evidence of hyperplasia was observed in stomachs of the 10–12-week-old $Atp4a^{-/-}$ mice, consistent with the lack of a significant increase in mitotic cells. Morphometric analysis of the gastric glands from adult $Atp4a^{+/+}$ and $Atp4a^{-/-}$ mice showed that the glandular thickness was similar in the two genotypes (400 ± 21 and 417 ± 35 μm, respectively; Table II). However, the thickness of the epithelial cell layer was significantly thinner in $Atp4a^{-/-}$ glands ($Atp4a^{+/+}$, 14.6 ± 0.6 μm; $Atp4a^{-/-}$, 8.9 ± 1.2 μm; $p < 0.05$; Table II). The decrease in the thickness of the epithelial layer in the $Atp4a^{-/-}$ glands was most likely attributable to the large dilations in the gastric gland lumen (Fig. 8, *B* and *C*), which pressed the cells against the basement membrane.

*Ultrastructure of Parietal and Chief Cells—*$Atp4a^{+/+}$ parietal cells had numerous mitochondria and extensive intracellular canaliculi densely packed with microvilli (Fig. 9*A*), and tubulovesicles were observed immediately adjacent to the canaliculi. In contrast, the $Atp4a^{-/-}$ parietal cells did not contain normal canaliculi; rather, they contained dilated canaliculi (Fig. 9*B*) with few, if any, of the microvilli typical of $Atp4a^{+/+}$ canaliculi (Fig. 9*A*). Present on the apical membrane of mutant parietal cells was a sparse population of short, dense microvilli (Fig. 9*B*), which were similar in appearance to the microvilli on the apical membrane of mucous and chief cells. Spherical vesicles, rather than normal tubulovesicles, were occasionally observed in $Atp4a^{-/-}$ parietal cells (Fig. 9*B*). Large cytoplasmic glycogen pools in $Atp4a^{-/-}$ parietal cells were also observed (Fig. 9*B*). Interestingly, some mitochondria in the $Atp4a^{-/-}$ parietal cells appeared enlarged and filled with concentric cristae (Fig. 9*C*) rather than the normal transverse cristae seen in mitochondria of $Atp4a^{+/+}$ parietal cells.

Electron micrographs showed chief cells with both secretory granules and rough endoplasmic reticulum in $Atp4a^{-/-}$ stomachs (Fig. 10). Subjectively, the numbers of granules and the amount of rough endoplasmic reticulum appeared to be decreased relative to those of wild-type cells, consistent with

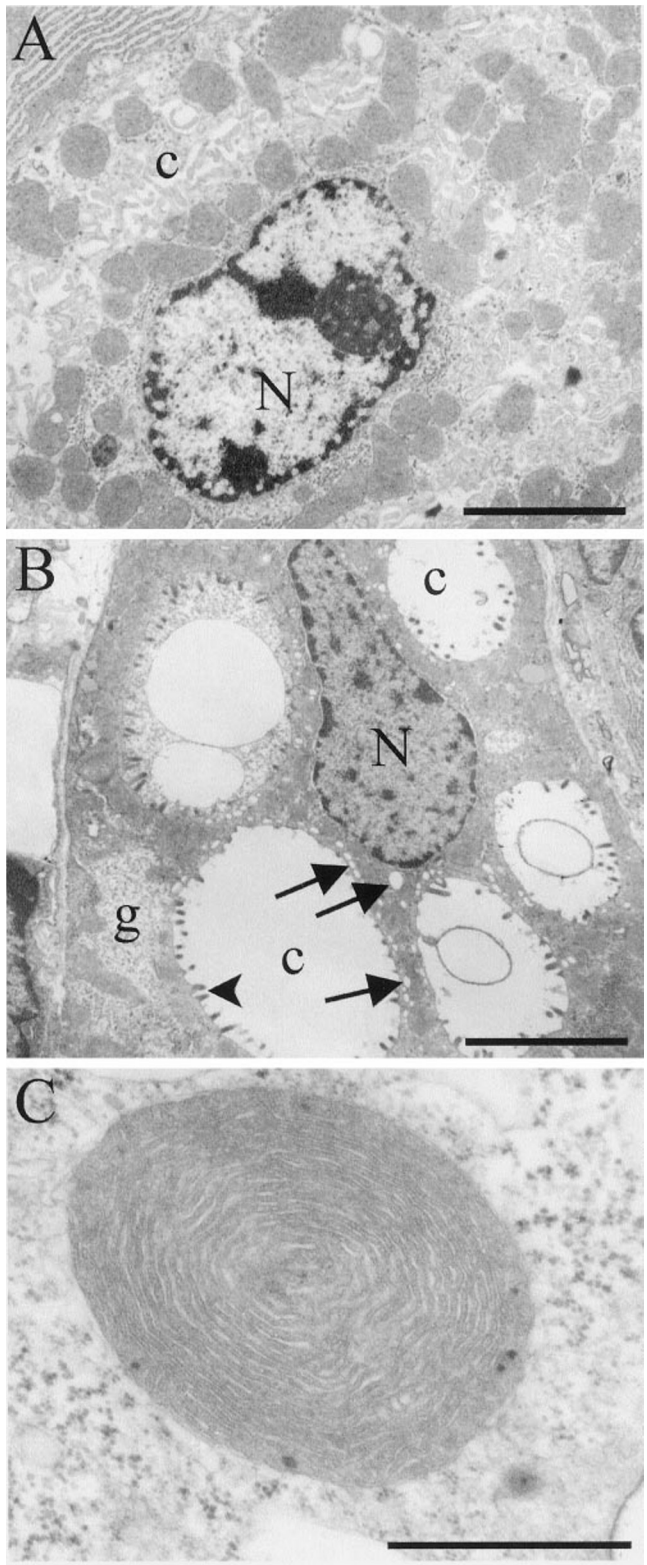


FIG. 9. **Electron micrographs of parietal cells in $Atp4a^{+/+}$ and $Atp4a^{-/-}$ stomachs.** *A*, parietal cell from an $Atp4a^{+/+}$ mouse, with well developed secretory canaliculus (*c*), nucleus (*N*), and many mitochondria. *B*, in the $Atp4a^{-/-}$ parietal cell, canaliculi were dilated, and microvilli of the canaliculus (*arrowheads*) were less abundant, shorter, and more densely stained than in wild-type cells. $Atp4a^{-/-}$ parietal cells contained a few rounded vesicles (*arrows*) rather than numerous tubulovesicles and accumulated glycogen (*g*). *C*, $Atp4a^{-/-}$ parietal cells often contained large mitochondria with concentric cristae. *Scale bars*, 5 μm (*A* and *B*) or 1 μm (*C*).


FIG. 10. **Electron micrograph of chief cell in *Atp4a*$^{-/-}$ stomach.** An example is shown of a well differentiated chief cell present in *Atp4a*$^{-/-}$ stomach. It should be noted that not all chief cells of *Atp4a*$^{-/-}$ stomachs were as well developed as the one shown here; in general, they had fewer secretory granules (*SG*) and less abundant rough endoplasmic reticulum (*RER*) than those found in wild-type stomachs. *Scale bar*, 5 $\mu$m.

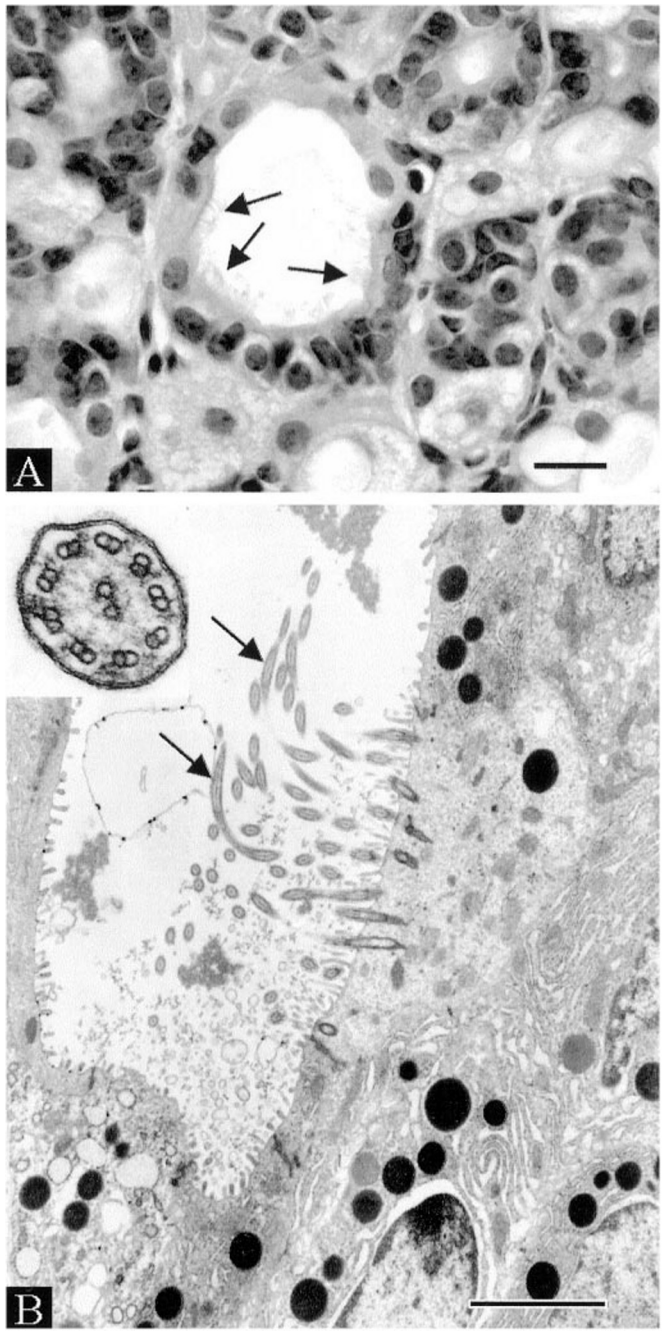


FIG. 11. **Ciliated metaplasia of *Atp4a*$^{-/-}$ stomach.** *A*, hematoxylin- and eosin-stained section of *Atp4a*$^{-/-}$ mouse stomach, showing cells with cilia on their apical membrane (*arrows*). Scale bar, 10 $\mu$m. *B*, electron micrograph of a ciliated cell from an *Atp4a*$^{-/-}$ stomach. Numerous cilia (*arrows*) project from the apical surface into the lumen of the gastric gland. The *inset* shows a cross-section of a cilia. *Scale bar*, 4 $\mu$m.

observations by light microscopy. Nevertheless, it was clear that mature chief cells with well developed secretory granules were produced in *Atp4a*$^{-/-}$ glands and that their numbers were relatively normal.

*Metaplasia in Atp4a*$^{-/-}$ *Stomachs*—In both toluidine blue- (data not shown) and in hematoxylin and eosin-stained sections of adult *Atp4a*$^{-/-}$ stomachs, cells with numerous distinct cilia located on the apical membrane and extending into the lumen of the gland were observed (Fig. 11*A*). Ciliated cells comprised 1.08 ± 0.45% of the epithelial cells counted in *Atp4a*$^{-/-}$ glands (Table II). In contrast, ciliated cells were seen only rarely in juvenile *Atp4a*$^{-/-}$ glands and were not observed in gastric glands of *Atp4a*$^{+/+}$ mice (Table II). Ciliated cells were observed in small cystically dilated regions of the gastric gland (Fig. 11*A*) and in the base of the gland and occurred both in clusters and singly. Ultrastructural analysis (Fig. 11*B*) revealed that the cilia had the typical structure of motile cilia. A central pair of microtubules, nine peripheral microtubule doublets, radial spokes connecting the central and peripheral microtubules, and dynein arms were apparent in cross-sections of the ciliary shaft (see *inset* of Fig. 11*B*), and the basal body contained the typical nine triplet microtubules (not shown).

Large irregularly shaped cysts were sometimes observed near the apex of the adult *Atp4a*$^{-/-}$ gastric gland in both toluidine blue-stained (Fig. 8*C*) and hematoxylin- and eosin-stained (data not shown) sections. These large cysts were lined with a single layer of epithelial cells, which were not immediately identifiable as a gastric epithelial cell type but had the appearance of a low cuboidal undifferentiated epithelial cell type. In hematoxylin and eosin-stained thick sections, cysts were often filled with cellular debris and mucous (data not shown), leading to the tentative identification of the surrounding epithelial cell layer as mucous cells.

Stomachs from 12-week-old *Atp4a*$^{+/+}$ and *Atp4a*$^{-/-}$ mice were stained with PAS/Alcian blue, which stains neutral carbohydrates red (PAS-positive) and acidic carbohydrates blue (Alcian blue-positive) and were examined by light microscopy. Mucous pit cells from *Atp4a*$^{+/+}$ mice stained red at the apical membrane (Fig. 12*A*). Most of the pit cells from *Atp4a*$^{-/-}$ mice stained red, but a few stained purple (Fig. 12*B*), indicating that they contained both neutral and acidic carbohydrates, and epithelial cells lining the cysts in the *Atp4a*$^{-/-}$ glands

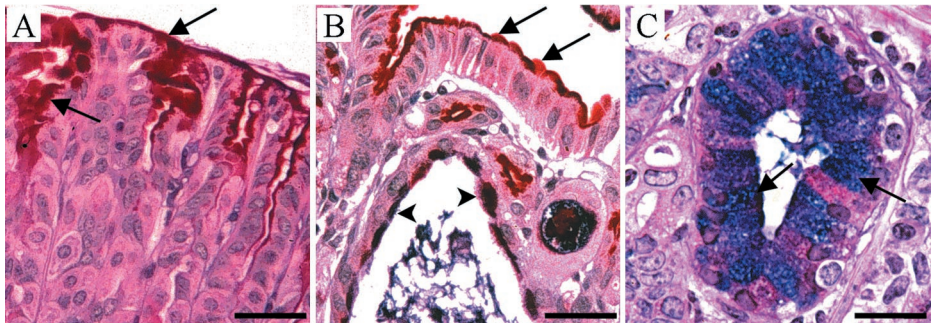


FIG. 12. **PAS/Alcian blue-stained stomach sections from *Atp4a*$^{+/+}$ and *Atp4a*$^{-/-}$ gastric glands.** Paraffin-embedded sections from adult mouse stomachs were stained with PAS and Alcian blue to analyze carbohydrate moieties. *A*, mucous cells in the apex of *Atp4a*$^{+/+}$ oxyntic glands stained *bright red* (*arrows*), indicating the presence of neutral polysaccharides. *B*, mucous cells in the apex of *Atp4a*$^{-/-}$ oxyntic glands exhibited the normal *red* staining (*arrows*), but mucous cells surrounding cystically dilated regions often stained *purple* (*arrowheads*), indicating the presence of both neutral and acidic polysaccharides. *C*, in addition to cells staining *red* or *purple*, a small cyst at the base of an *Atp4a*$^{-/-}$ gastric gland contained cells that stained *blue* (*arrows*), indicating the presence of acidic polysaccharides and the absence of neutral polysaccharides. *Scale bars*, 50 $\mu$m (*A* and *B*) or 20 $\mu$m (*C*).

also stained dark purple (Fig. 12*B*). Fig. 12*C* shows a small dilation at the base of a *Atp4a*$^{-/-}$ gland lined with PAS-positive (red), Alcian blue-positive (blue), and PAS/Alcian blue-positive (purple) cells. These data indicate that some mucous cells in *Atp4a*$^{-/-}$ gastric glands produce and secrete modified mucosubstances.

## DISCUSSION

In preparing the gastric H,K-ATPase $\alpha$-subunit-deficient mouse, we deleted sequences in exon 8 encoding the catalytic phosphorylation site, which is critical for enzyme activity, and inserted the neomycin resistance gene. Northern blot analysis demonstrated that the mutation eliminated expression of the $\alpha$-subunit mRNA, and immunostaining of sections from *Atp4a*$^{-/-}$ stomachs showed that $\alpha$-subunit protein was also absent. These data confirmed that the targeting procedure had produced a null mutation. Homozygous mutant mice were born in a normal Mendelian ratio and appeared healthy, indicating that the gastric H,K-ATPase $\alpha$-subunit is not required for embryonic development or for viability of the animal during the time period studied.

On the basis of its expression in mouse kidney and the occurrence of $HCO_3^-$ reabsorption in the collecting duct that is sensitive to SCH28080, an inhibitor of the gastric H,K-ATPase, it seemed possible that this enzyme might play a role in the maintenance of systemic acid-base homeostasis (19, 20). However, analysis of blood from adult mutant and wild-type mice revealed no significant perturbation of acid-base balance. Normal acid-base status was observed previously in mice lacking the colonic H,K-ATPase (25), which is also expressed in kidney. Thus, neither of the known H,K-ATPase isoforms is necessary for systemic acid-base homeostasis when mice are maintained under normal conditions. In contrast, the B1 subunit of the V-type $H^+$-ATPase clearly functions in renal control of acid-base homeostasis, since null mutations in its gene have been shown to cause distal renal tubular acidosis in humans (26). Whether gastric H,K-ATPase activity in the collecting duct can provide partial compensation when an animal is subjected to systemic acidosis remains to be determined.

Expression of the H,K-ATPase $\alpha$-subunit was eliminated in *Atp4a*$^{-/-}$ stomachs, but mRNA encoding the $\beta$-subunit was increased and $\beta$-subunit protein was easily detected in *Atp4a*$^{-/-}$ parietal cells. Thus, the H,K-ATPase-deficient mouse described here differs from that prepared by van Driel and colleagues (7), in which the $\beta$-subunit gene was targeted. In that model, expression of the $\beta$-subunit was eliminated, and expression of the $\alpha$-subunit was reduced to very low levels.

A stomach phenotype similar to that reported for mice lacking the H,K-ATPase $\beta$-subunit (7) (*i.e.* achlorhydria, hypergastrinemia, and histopathologic changes in the gastric mucosa) was observed in $\alpha$-subunit-deficient mice. Achlorhydria and hypergastrinemia were expected, since achlorhydria is consistent with the established role of the H,K-ATPase $\alpha$-subunit in acid secretion, and hypergastrinemia is known to occur as a result of achlorhydria. In both knockouts, parietal cells develop and are present at normal numbers in adult stomachs, but they lack tubulovesicles and contain dilated canaliculi rather than a normal secretory canaliculus. These observations suggest that both subunits are necessary for biogenesis of the secretory membranes.

Although the phenotypes of the two H,K-ATPase-deficient mice are similar in many respects, there appear to be significant differences as well. Gastric mucosal hypertrophy, mononuclear cells in the lamina propria and submucosal regions, and a reduction in the number of chief cells were observed in mice lacking the $\beta$-subunit (7) but not in those lacking the $\alpha$-subunit. In both mice, the dilated canaliculi become more prominent with age; however, this defect did not seem as severe in mice lacking the $\alpha$-subunit as in those lacking the $\beta$-subunit. Also, in $\beta$-subunit-deficient mice, the dilated canaliculi, which were often massive and caused the cells to be severely swollen, were reported to be invariably intracellular (7), whereas the dilated canaliculi in the $\alpha$-subunit knockout were not as prominent and appeared to be continuous with the lumen of the gland. Whether these differences are due to the loss of different subunits or are due to differences in genetic background or other factors is unclear. It is known that the $\beta$-subunit is necessary for delivery of the $\alpha$-subunit to the plasma membrane (7, 27) and that it has a sequence involved in endocytic retrieval of the pump (5). Furthermore, the $\beta$-subunit can attain cell surface expression in the absence of the $\alpha$-subunit (27), and a population of $\beta$-subunit monomers has been identified in the parietal cell (28). Thus, it is conceivable that the $\beta$-subunit is necessary not only for endocytic retrieval, which is intimately involved in the transition from the stimulated to the resting state (5), but also for recruitment of secretory membranes to the apical membrane of the parietal cell. If this hypothesis is correct, then the mechanism for incorporating secretory membranes into the apical membrane of the parietal cell may be deficient in the $\beta$-subunit knockout but largely intact in the $\alpha$-subunit knockout, which expresses significant levels of $\beta$-subunit. With stimulated secretion occurring via $K^+$ and $Cl^-$ channel activities, the dilated canaliculi would tend to become enlarged in $\beta$-subunit-deficient parietal cells, due to the lack of an outlet for accumulated fluid, but less distended in

those lacking the α-subunit, in which the canaliculi appear to be continuous with the lumen of the gland.

Abnormally large mitochondria with concentric cristae and massive glycogen stores were observed in a subset of parietal cells from 10–12-week-old α-subunit-deficient mice. Mitochondria with concentric cristae have been observed in respiratory chain disorders (29–31) or after treatment with toxins (32) that inhibit mitochondrial activity. The absence of H,K-ATPase activity and reduced transepithelial transport in α-subunit-deficient parietal cells would be expected to cause a sharp reduction in cellular ATP utilization. It is possible that the occurrence of abnormal mitochondria in *Atp4a*$^{-/-}$ parietal cells is due to low mitochondrial activity secondary to sharply reduced cellular ATP utilization, which would be expected to occur as a result of the loss of H,K-ATPase activity and reduced transepithelial transport. The accumulation of glycogen could also be due to decreased energy utilization by the parietal cell. This interpretation must be considered with caution because altered mitochondria and increased glycogen stores were not reported in β-subunit-deficient parietal cells, which should have the same deficit in energy utilization. This difference, however, may be due to the relatively young age (35 days) of the β-subunit-deficient mice that were studied (7).

When animals are treated with omeprazole, an H,K-ATPase inhibitor, their parietal cells develop dilated canaliculi and undergo an increased rate of degeneration, invasion by macrophages occurs, and the preparietal cell population increases (8). Karam and Forte (8) suggested the possibility that complete and extended inhibition of acid secretion might be sufficient to cause parietal cell degeneration. A potential mechanism is that a block in the secretion of acid across the apical membrane might be detrimental to cells in which the transport processes on the basolateral membrane are being stimulated, since such an imbalance might cause severe perturbations of intracellular pH and volume homeostasis. Along these lines, it has been proposed that the parietal cell degeneration observed in mice lacking the NHE2 $Na^+/H^+$ exchanger might be due to cell volume perturbations secondary to a deficiency in $Na^+/H^+$ exchange across the basolateral membrane during active acid secretion (16). *Atp4a*$^{-/-}$ mice developed dilated canaliculi that are similar in appearance to those of omeprazole-treated animals; however, there was no evidence of an increased rate of degeneration or production of parietal cells. The number of parietal cells was essentially the same in mutant and wild-type mice; there appeared to be little, if any, increase in the number of preparietal cells or inflammatory cells; and the number of mitotic cells was essentially the same. These results suggest that the viability of α-subunit-deficient parietal cells is not seriously affected by an imbalance between apical and basolateral transport processes; they also demonstrate that parietal cells containing dilated caniculi and lacking the ability to secrete gastric acid can, nevertheless, remain viable. Thus, the degeneration of the modified parietal cells observed previously after treatment with omeprazole must be due to factors other than the loss of acid secretion. One possibility is that covalent modification of the pump might lead to cell injury (discussed in Ref. 8), as observed in Clara cells of the lung after covalent binding of 4-ipomeanol to cellular proteins (29).

A second major difference between the gastric mucosa of *Atp4a*$^{-/-}$ mice and that of animals treated with omeprazole is that long term omeprazole treatment leads to a sharp reduction in the number of mature chief cells (9), whereas only a small decrease in chief cells, which was not statistically significant, was observed in adult *Atp4a*$^{-/-}$ mice. An apparent block in the maturation of chief cells has been observed in several achlorhydric mouse lines, including NHE2 $Na^+/H^+$ exchanger-deficient mice (16), mice in which mature parietal cells were ablated by expression of diphtheria toxin (13), and mice in which the simian virus 40 T antigen was expressed in parietal cells (14). In addition to the loss of acid secretion, other common phenotypic characteristics of these mice and of omeprazole-treated animals, which did not occur in *Atp4a*$^{-/-}$ mice, were the loss of mature parietal cells and an expansion of the preparietal cell population. Because substantial numbers of mature chief cells were observed in *Atp4a*$^{-/-}$ mice, it is clear that achlorhydria does not cause a major block in their differentiation. Li *et al.* (14) suggested the alternative possibilities that differentiation of chief cells might be affected by the loss of a positive factor that is normally produced by mature parietal cells or by the production of an inhibitory factor by an expanded preparietal cell population. The results of the current study are consistent with either of these possibilities, since we observed normal numbers of viable parietal cells in *Atp4a*$^{-/-}$ mice and no evidence of an increase in the number of preparietal cells.

Despite the presence of relatively normal numbers of chief cells, with secretory granules containing pepsinogen, pepsinogen mRNA in *Atp4a*$^{-/-}$ stomachs was sharply reduced relative to that of *Atp4a*$^{+/-}$ and *Atp4a*$^{+/+}$ stomachs. It is unlikely that this was due to a general reduction in mRNA synthesis or abundance in chief cells, because normal levels of intrinsic factor mRNA were expressed in *Atp4a*$^{-/-}$ stomachs. Given the very low levels of pepsinogen mRNA and the apparent abundance of pepsinogen in *Atp4a*$^{-/-}$ chief cells, it appears likely that pepsinogen synthesis and secretion are sharply reduced. Treatment of rats with concentrations of omeprazole sufficient to inhibit acid secretion has been shown to cause a decrease in pepsinogen mRNA, accumulation of pepsinogen in secretory granules, and inhibition of pepsinogen secretion (33). It was unclear, however, whether the observed results were due to a direct effect of omeprazole on chief cells or were secondary to achlorhydria or other alterations occurring in the gastric mucosa of omeprazole-treated animals. The results of the current study suggest that achlorhydria itself may cause inhibition of pepsinogen secretion and down-regulation of the pepsinogen gene.

A number of metaplastic changes were observed in *Atp4a*$^{-/-}$ gastric glands. These included cystically dilated regions lined with a relatively undifferentiated cuboidal cell type (Fig. 8*C*) and the presence of both ciliated cells (Fig. 11) and altered mucous cells (Fig. 12) that produced acidic carbohydrate moieties not normally seen in gastric mucous cells. In humans, ciliated metaplasia has been observed occasionally in Caucasians (34), but it occurs more frequently in people of Japanese and Polynesian descent (35–37). When observed, ciliated metaplasia generally occurs in cystically dilated glands and is associated with dysplasia and intestinal metaplasia (34–38). There is suggestive evidence for an association between ciliated metaplasia and stomach cancer (35, 38). In *Atp4a*$^{-/-}$ mice, ciliated metaplasia occurred in cystically dilated glands and was associated with dysplasia, but we have not observed intestinal metaplasia or cancer in the mice studied so far. The mechanistic basis for the metaplastic changes in *Atp4a*$^{-/-}$ stomachs is unclear.

In summary, our results confirm that the gastric H,K-ATPase is essential for acid secretion; however, a number of our major findings are contrary to what was anticipated on the basis of previous studies. First, biogenesis of the secretory membranes was altered, but there were noteworthy differences when compared with the alterations observed in the β-subunit knockout (7). The phenotypic differences between the two knockouts suggest that the β-subunit is necessary and sufficient for incorporation of secretory membranes into the apical

membrane of the parietal cell. Second, unlike the effects of omeprazole treatment, elimination of the $\alpha$-subunit did not impair parietal cell viability, and there was little, if any, expansion of the preparietal cell population or impairment of chief cell differentiation. Also, we observed metaplastic changes that were not reported after treatment with inhibitors of acid secretion or ablation of the $\beta$-subunit. Gordon and colleagues (13) presented strong evidence that the mature parietal cell plays a critical role in terminal differentiation of the various gastric epithelial cell types. Our results are consistent with the possibility that the mature *Atp4a*$^{-/-}$ parietal cell, despite its inability to secrete gastric acid, can provide inputs needed for relatively normal differentiation of gastric epithelial cells but that perturbations of the instructive signals and the absence of the normal acidic milieu of the gastric gland either promote or are permissive for metaplastic changes. In future studies, the *Atp4a*$^{-/-}$ mouse should be a useful *in vivo* model for studying secretory membrane biogenesis and the role of the parietal cell in differentiation and maturation of gastric epithelial cells.

REFERENCES


1. Chow, D. C., and Forte, J. G. (1995) *J. Exp. Biol.* **198,** 1–17
2. Shull, G. E., and Lingrel, J. B. (1986) *J. Biol. Chem.* **261,** 16788–16791
3. Shull, G. E. (1990) *J. Biol. Chem.* **265,** 12123–12126
4. Dunbar, L. A., Courtois-Coutry, N., Roush, D. L., Muth, T. R., Gottardi, C. J., Rajendran, V., Geibel, J., Kashgarian, M., and Caplan, M. J. (1998) *Acta Physiol. Scand.* **163,** Suppl. 643, 289–295
5. Courtois-Coutry, N., Roush, D., Rajendran, V., McCarthy, J. B., Geibel, J., Kashgarian, M., and Caplan, M. J. (1997) *Cell* **90,** 501–510
6. Forte, J. G., and Yao, X. (1996) *Trends Cell Biol.* **6,** 45–48
7. Scarff, K. L., Judd, L. M., Toh, B.-H., Gleeson, P. A., and van Driel, I. R. (1999) *Gastroenterology* **117,** 605–618
8. Karam, S. M., and Forte, J. G. (1994) *Am. J. Physiol.* **266,** G745–G758
9. Kakei, N., Ichinose, M., Tatematsu, M., Shimizu, M., Oka, M., Yahagi, N., Matsushima, M., Kurokawa, K., Yonezawa, S., Furihata, C., Shiokawa, K., Kageyama, T., Miki, K., and Fukamachi, H. (1995) *Biochem. Biophys. Res. Commun.* **214,** 861–868
10. Lehy, T., and Dubrasquet, M. (1972) *Am. J. Dig. Dis.* **17,** 887–901
11. Karasawa, H., Tani, N., and Miwa, T. (1988) *Gastroenterol. Jap.* **23,** 1–8
12. Helander, H. F., Mattsson, H., Elm, G., and Ottosson, S. (1990) *Scand. J. Gastroenterol.* **25,** 799–809
13. Li, Q., Karam, S. M., and Gordon, J. I. (1996) *J. Biol. Chem.* **271,** 3671–3676
14. Li, Q., Karam, S. M., and Gordon, J. I. (1995) *J. Biol. Chem.* **270,** 15777–15788
15. Mathews, P. M., Claeys, D., Jaisser, F., Geering, K., Horisberger, J.-D., Kraehenbuhl, J.-P., and Rossier, B. C. (1995) *Am. J. Physiol.* **268,** C1207–C1214
16. Schultheis, P. J., Clarke, L. L., Meneton, P., Harline, M., Boivin, G. P., Stemmermann, G., Duffy, J. J., Doetschman, T., Miller, M. L., and Shull, G. E. (1998) *J. Clin. Invest.* **101,** 1243–1253
17. Stechschulte, D. J., Jr., Morris, D. C., Jilka, R. L., and Dileepan, K. N. (1990) *Am. J. Physiol.* **259,** G41–G47
18. Church, G. M., and Gilbert, W. (1984) *Proc. Natl. Acad. Sci. U. S. A.* **81,** 1991–1995
19. Nakamura, S., Amlal, H., Schultheis, P. J., Galla, J. H., Shull, G. E., and Soleimani, M. (1999) *Am. J. Physiol.* **276,** F914–F921
20. Silver, R. B., and Soleimani, M. (1999) *Am. J. Physiol.* **276,** F799–F811
21. Brand, S. J., and Schmidt, W. E. (1995) in *Gastroenterology*, 2nd Ed. (Yamada, T., ed) pp. 25–71, J.B. Lippincott Co., Philadelphia
22. Langhans, N., Rindi, G., Chiu, M., Rehfeld, J. F., Ardman, B., Beinborn, M., and Kopin, A. S. (1997) *Gastroenterology* **112,** 280–286
23. Lorenz, R. G., and Gordon, J. I. (1993) *J. Biol. Chem.* **268,** 26559–26570
24. Maeda, M., Asahara, S., Nishi, T., Mushiake, S., Oka, T., Shimada, S., Chiba, T., Tohyama, M., and Futai, M. (1995) *J. Biochem.* (*Tokyo*) **117,** 1305–1311
25. Meneton, P., Schultheis, P. J., Greeb, J., Nieman, M. L., Liu, L., Clarke, L. L., Duffy, J. J., Doetschman, T., Lorenz, J. N., and Shull, G. E. (1998) *J. Clin. Invest.* **101,** 536–542
26. Karet, F. E., Finberg, K. E., Nelson, R. D., Nayir, A., Mocan, H., Sanjad, S. A., Rodriguez-Soriano, J., Santos, F., Cremers, C. W. R. J., Di Pietro, A., Hoffbrand, B. I., Winiarski, J., Bakkaloglu, A., Ozen, S., Dusunsel, R., Goodyer, P., Hulton, S. A., Wu, D. K., Skvorak, A. B., Morton, C. C., Cunningham, M. J., Jha, V., and Lifton, R. P. (1999) *Nat. Genet.* **21,** 84–90
27. Gottardi, C. J., and Caplan, M. J. (1993) *J. Biol. Chem.* **268,** 14342–14347
28. Baldwin, G. S. (1990) *FEBS Lett.* **272,** 159–162
29. Behbehani, A. W., Goebel, H., Osse, G., Gabriel, M., Langenbeck, U., Berden, J., Berger, R., and Schutgens, R. B. H. (1984) *Eur. J. Pediatr.* **143,** 67–71
30. Hoppel, C. L., Kerr, D. S., Dahms, B., and Roessmann, U. (1987) *J. Clin. Invest.* **80,** 71–77
31. DiMauro, S., Mendell, J. R., Sahenk, Z., Bachman, D., Scarpa, A., Scofield, R. M., and Reiner, C. (1980) *Neurology* **30,** 795–804
32. Shah, A. J., Sahgal, V., Muschler, G., Subramani, V., and Singh, H. (1982) *J. Neurol. Sci.* **55,** 25–37
33. Kakei, N., Ichinose, M., Tsukada, S., Tatematsu, M., Tezuka, N., Yahagi, N., Matsushima, M., Miki, K., Kurokawa, K., Takahashi, K., and Fukamachi, H. (1993) *Biochem. Biophys. Res. Commun.* **195,** 997–1004
34. Rubio, C. A., and Antonioli, D. (1988) *Am. J. Surg. Pathol.* **12,** 786–789
35. Rubio, C. A., and Kato, Y. (1986) *Jpn. J. Cancer Res.* **77,** 282–286
36. Rubio, C. A., Stemmermann, G. N., and Hayashi, T. (1991) *Jpn. J. Cancer Res.* **82,** 86–89
37. Rubio, C. A., Jass, J. R., and King, A. (1994) *J. Environ. Pathol. Toxicol. Oncol.* **13,** 243–249
38. Chan, W. Y., Hui, P. K., Leung, K. M., Robertson, C. S., and Chung, S. C. S. (1993) *Hum. Pathol.* **24,** 1107–1113